



Copyright © 2013, Paper 17-019; 52558 words, 12 Figures, 0 Animations, 6 Tables.
<http://EarthInteractions.org>

Climate Change Effects on Hydropower Potential in the Alcantara River Basin in Sicily (Italy)

G. T. Aronica* and B. Bonaccorso

Dipartimento di Ingegneria Civile, Informatica, Edile, Ambientale e Matematica Applicata, Università di Messina, Messina, Italy

Received 5 December 2012; accepted 11 May 2013

ABSTRACT: In recent years, increasing attention has been paid to hydropower generation, since it is a renewable, efficient, and reliable source of energy, as well as an effective tool to reduce the atmospheric concentrations of greenhouse gases resulting from human activities. At the same time, however, hydropower is among the most vulnerable industries to global warming, because water resources are closely linked to climate changes. Indeed, the effects of climate change on water availability are expected to affect hydropower generation with special reference to southern countries, which are supposed to face dryer conditions in the next decades. The aim of this paper is to qualitatively assess the impact of future climate change on the hydrological regime of the Alcantara River basin, eastern Sicily (Italy), based on Monte Carlo simulations. Synthetic series of daily rainfall and temperature are generated, based on observed data, through a first-order Markov chain and an autoregressive moving average (ARMA) model, respectively, for the current scenario and two future scenarios at 2025. In particular, relative changes in the monthly mean and standard deviation values of daily rainfall and temperature at 2025, predicted by the Hadley Centre Coupled Model, version 3 (HadCM3) for A2 and B2 greenhouse gas emissions scenarios, are adopted to generate future values of precipitation and

* Corresponding author address: G. T. Aronica, Dipartimento di Ingegneria Civile, Informatica, Edile, Ambientale e Matematica Applicata, Università di Messina, Strada Panoramica dello Stretto, 98166 S. Agata, Messina, Italy.

E-mail address: garonica@unime.it

temperature. Synthetic series for the two climatic scenarios are then introduced as input into the Identification of Unit Hydrographs and Component Flows from Rainfall, Evapotranspiration and Streamflow Data (IHACRES) model to simulate the hydrological response of the basin. The effects of climate change are investigated by analyzing potential modification of the resulting flow duration curves and utilization curves, which allow a site's energy potential for the design of run-of-river hydropower plants to be estimated.

KEYWORDS: Hydropower; Climate change; IHACRES; Monte Carlo analysis; Mediterranean areas; Sicily

1. Introduction

In recent years, an increasing attention has been paid to hydropower generation, since it is a renewable, efficient, and reliable source of energy, as well as an asset to reduce the atmospheric concentrations of greenhouse gases resulting from human activities. At the same time, however, hydropower is among the most vulnerable industries to global warming, because water resources are closely linked to climate changes. Indeed, the effects of climate change on water availability are expected to affect hydropower generation. Climate change will most likely increase the frequency of droughts and water scarcity in some areas, such as southern and southeastern parts of Europe, which already suffer water stress (Bernstein et al. 2007).

Particularly interesting, as important indicators of global warming, are the projected trends of climate variables such as temperature and rainfall on the Mediterranean area. In this region, according to Christensen et al. (Christensen et al. 2007), annual mean temperatures will rise more than the global average and the warming is likely to be largest in summer. Moreover, the majority of the general circulation models (GCMs) foresee an increase, in frequency, of extreme daily precipitation, despite a decrease in total values. Thus, this tendency can lead to longer dry periods, increasing the risks of droughts, interrupted by extreme intense precipitation, enhancing the flood risk (Bates et al. 2008).

Average runoff in southern European rivers is projected to decrease with increasing temperatures and decreasing precipitation. In particular, some river basins in the Mediterranean regions may see decreases of 10% or more below today's levels by 2030.

The objective of this study is to qualitatively investigate the effects of predicted short-term climate change scenarios on hydropower potential of the Alcantara River basin, located in the eastern part of Sicily, Italy. The interest in this case study is twofold: on the one hand, it represents the main river natural park in Sicily and, on the other hand, its water resources supply different users. Therefore, the need arises to guarantee an appropriate balance between in-stream water uses, such as ecosystem maintenance and hydropower generation, and water withdrawals, which are essential for socioeconomic development of the area, also in view of possible modification in water resources availability due to climate change.

In addition, since hydropower generation through run-of-river plants, as is the case of the present study, is more vulnerable than impoundment hydropower plants to alteration of rainfall and temperature regimes due to climate change, there is a further interest in modeling approaches for forecasting flow regimes of the Alcantara River under different climatic conditions. To this end, the emphasis of this study is placed

on determining and comparing flow duration curves (FDCs), as well as the resulting utilization curves, for current and future scenarios.

One of the most common approaches that are used to study the potential impact of climate change on the hydrology and water resources of a river basin lies in applying the projections obtained from GCMs, either directly or by downscaling to the appropriate river basin scale, through regional climate models (RCMs). Because of their coarse spatial resolution, which is seldom as fine as $2.5^\circ \times 2.5^\circ$, GCMs are usually applied to study the impact of climate change on the hydrology of major river basins, which cover a reasonable number of GCM grid cells (Arora and Boer 2001; Mirza 2002; Hamlet and Lettenmaier 2007; Gain et al. 2011).

On the other hand, GCMs are inadequate to simulate regional and local climate change when dealing with spatial scale of $\sim 1000 \text{ km}^2$ or finer, as in most common hydrological applications. Therefore, downscaling or disaggregating techniques (both statistical methods and nested RCMs) are generally used to transfer climate data from GCM scales to the river basin scale (Xu 1999; Wilby et al. 2004; Hanssen-Bauer et al. 2005; Fowler et al. 2007; Teutschbein and Seibert 2012).

The last step to assess the effects of climate change on the hydrologic regime of a river basin consists in inputting the results of statistical downscaling models or of RCMs into hydrological models able to simulate flow regime at the river basin scale accurately (Aronica et al. 2005; Candela et al. 2009). It is worth pointing out that this methodology is characterized by various uncertainties. One of the major sources of uncertainty stems from the downscaling and bias correction techniques, also with respect to the resolution of the hydrological model (Kunstmann et al. 2004; Kunstmann and Stadler 2005; Dibike and Coulibaly 2005; Prudhomme and Davies 2009; Quintana Seguí et al. 2010; Senatore et al. 2011). In particular, typical resolution of RCMs ranges between 20 and 50 km, which is still unsuitable for impact studies on relatively small river basins, as many of those located in Mediterranean regions.

An alternative approach for impact analysis consists in extrapolating future behavior from past observations based on detected changes (e.g., trends and/or jumps) in historical records. More specifically, the identified patterns, which must be adjusted as long as new observations become available over time, can be applied for future predictions.

Although this approach is apparently easier and less uncertain than the one based on GCMs predictions, it is worth pointing out that its reliability is strictly related to the length and quality of available datasets. In particular, unreliable results can be derived when the historical records are either too short (e.g., less than 30 years) or long enough but fragmented by several periods of missing data.

Therefore, a scenario-based approach, based on the GCMs predictions, could be considered a fair alternative in case when an impact analysis has to be carried out in a region characterized by daily weather data scarcity, as is the case presented here. Clearly, it is worth bearing in mind that the outputs of such model should be seen as rough estimates of possible future conditions, which can help decision makers to plan adapting strategies for water resources management.

Given the small size of the study area (about 400 km^2), in the present study no attempt has been made to make use of RCMs. Rather, the potential hydrological impacts of climate change on water resources availability are estimated by changing the climate inputs (i.e., temperature and precipitation) to a rainfall–runoff model,

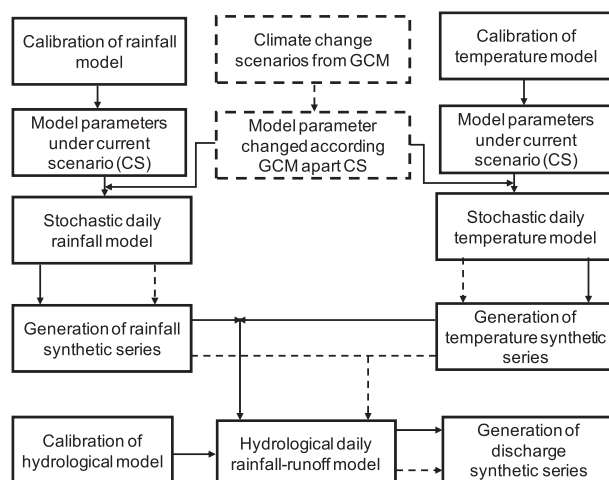


Figure 1. Flowchart showing the generation procedure.

following a stochastic approach. More specifically, synthetic series of daily rainfall and temperature series are generated based on appropriate stochastic models, whose parameters are first assessed by means of historic data. Those series are used as input to the adopted rainfall–runoff model in order to derive synthetic runoff series for the current climatic scenario.

Then, the parameters of daily rainfall and temperature stochastic models are computed once again based on the statistics (e.g., mean and standard deviation) of two climate change scenarios derived by a GCM model. Hence, new time series of daily temperature and precipitation are generated and inputted to the rainfall–runoff model to simulate time series of daily runoff under future scenarios. These steps are synthesized in the flowchart reported in Figure 1.

Finally, synthetic runoff series for the current and future scenarios are used to derive the corresponding flow duration curves and utilization curves, which are generally used to estimate a site’s energy potential for designing run-of-rivers hydropower plants (Mays 2001).

In the next section, the study area and the stochastic rainfall and temperature models, as well as the rainfall–runoff models, are presented in detail. Section 3 reports the description of climate change scenarios for the area under investigation. Then, the results of models calibration and validation are shown for both the current and future scenarios. Hence, a comparison is presented between the resulting flow duration curves and utilization curves aimed at evaluating the effects of changes in temperature and precipitation on hydropower potential of the river basin. Finally, conclusions about the proposed methodology, based on the derived results, are drawn in the last section.

2. Data and methods

2.1. Study area and data

The study area is part of the Alcantara River basin, located in the eastern side of Sicily (Figure 2). In particular, simulations are carried out with reference to the

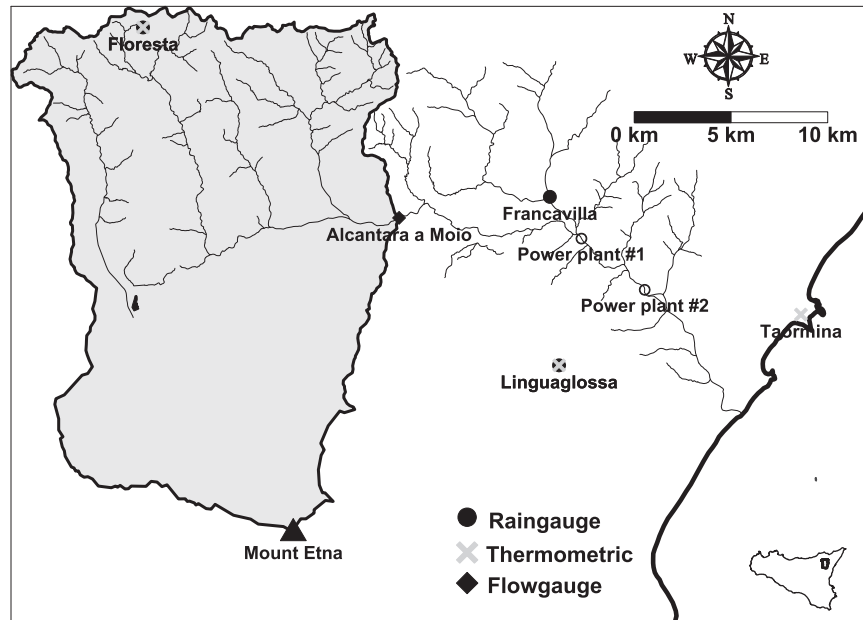


Figure 2. Layout of Alcantara River basin at the closing section of Alcantara a Moio.

Alcantara River basin at the closing section of Alcantara a Moio, whose extension is about 384 km^2 ($\sim 63\%$ of the total area at the river mouth). The main river channel length until Moio is about 30 km.

The river rises from the Nebrodi Mountains in Messina and flows through the foothills of the Nebrodi and Peloritani Mountains to the north and the volcanic massif of Etna Mountain to the south. The basin is partially covered with grassland located at the top hills and arable lands at the southeastern part.

The altitude of the Alcantara River basin varies from a maximum of 3274 m above MSL to 0 m above MSL at the river mouth, with mean annual temperature ranging from 15°C inland to 18°C on the coast. Mean annual precipitation over the basin is about 950 mm. Mean annual values of potential and effective evapotranspiration are about 780 and 460 mm, respectively.

The climate of the river basin can be classified as subhumid–humid, following Thornthwaite (Thornthwaite 1948). Mean annual flow is about $150.1 \text{ Mm}^3 \text{ yr}^{-1}$, whereas the available groundwater resources amount to $\sim 103 \text{ Mm}^3 \text{ yr}^{-1}$.

The middle valley of the Alcantara River is characterized by perennial surface flows enriched by spring water arising from the big aquifer of the Etna volcano. Groundwater recharge is mainly due to the amount of precipitation (both snow and rainfall) falling on the northwestern side of Etna Mountain, which, once infiltrated into the ground, percolates deeper. Based on previous geological studies on the Alcantara River basin (Di Marco and Licciardello 2005), it has been assessed that about 50 km^2 of the basin to the north of the Moio section contributes to base runoff. Such an area has been disregarded in the hydrologic modeling, which is oriented to simulate surface runoff only.

Water uses in the Alcantara River basin include municipal drinking water use (52%), agricultural use (30%), and industrial use (18%). In addition, surface water is diverted in two sections for hydropower generation through two run-of-river facilities operated by Enel Green Power, both located to the south of the Moio section (Figure 2).

The measurement network consists of three rain gauges (Floresta, Francavilla di Sicilia, and Linguaglossa), three thermometric stations (Floresta, Linguaglossa, and Taormina), and one flow gauge (Alcantara a Moio). In particular, the observation periods considered are as follows: 1967–2006 for daily rainfall series, 1981–88 for mean daily temperature series, and 1984–88 for mean daily discharge series.

It is worth specifying that, although daily precipitation datasets span over 40 years, the presence of various sequences of missing data prevents the derivation of plausible patterns that can support prediction of future values.

2.2. HadCM3 ocean-atmosphere general circulation model

The ocean-atmosphere general circulation model used to derive results in this work is the Hadley Centre Coupled Model, version 3 (HadCM3), which is widely used in climate change studies and extensively described in Gordon et al. (Gordon et al. 2000), Pope et al. (Pope et al. 2000), and Johns et al. (Johns et al. 2003). The choice of such a GCM model relies on the fact that it was widely used in climate change studies by the Intergovernmental Panel on Climate Change (IPCC) Third Assessment Report.

The atmospheric component of the model has a horizontal resolution of $2.5^\circ \times 3.75^\circ$, equivalent to a spatial resolution of $278 \text{ km} \times 295 \text{ km}$ in the latitudes of interest ($\sim 45^\circ$) with 19 vertical levels. The oceanic component of the model has 20 vertical levels with an horizontal resolution of $1.25^\circ \times 1.25^\circ$, which allows representing important details in the oceanic current structures.

Estimated greenhouse effect concentration gases for the medium-high A2 and medium-low B2 scenarios (Nakícenovíc 2000) were used as the global radiative forcing for the performance of the runs with reference to the period between 2013 and 2037, referred to here as 2025. The choice of this period was made by considering that results for this time horizon are more reliable than longer-term climate predictions.

2.3. Stochastic daily rainfall generation model

A simple stochastic daily rainfall generator, based on a Markov chain, is developed to derive synthetic series under different climatic scenarios. The model applied is a well-known chain-dependent-process stochastic model for daily precipitation structured in a two-state architecture (Gabriel and Neumann 1962; Todorovic and Woolhiser 1976; Haan et al. 1976; Waymire and Gupta 1981; Stern and Coe 1984; Wilks 1998): a first-order nonstationary Markov chain for modeling the rainfall occurrences and a probabilistic model for modeling the rainfall volumes. This model has been selected based on its mathematical simplicity and on the possibility of a robust calibration even with short-length rainfall samples. Further, the model is capable to incorporate trend effects in rainfall and consequently to generate series with statistical properties influenced by climate change.

Let X_t be a Bernoulli process representing the occurrence of a dry day or a wet day at day t , such that

$$X_t = \begin{cases} 0 & \text{if day } t \text{ is dry} \\ 1 & \text{if day } t \text{ is wet} \end{cases} \quad (1)$$

In what follows, $X_t = 1$ if at least a rainfall depth of 1 mm is observed at day t . The rainfall series is then

$$Y_t = h_t X_t, \quad (2)$$

where h_t represents the nonzero precipitation amounts.

The first-order Markov chain model for X_t follows from the assumption that

$$P(X_t = j_t | X_{t-1} = j_{t-1}, X_{t-2} = j_{t-2}, X_{t-3} = j_{t-3}, \dots) = P(X_t = j_t | X_{t-1} = j_{t-1}), \quad (3)$$

which states that the probability of a value of X at a given time t conditioned on past values, depends on the value of X at time $t - 1$ only.

Because X_t has a Markov chain structure, its joint probability distribution is determined uniquely once the transition probability matrix is defined: namely,

$$\begin{pmatrix} p_{00} & p_{01} \\ p_{10} & p_{11} \end{pmatrix}, \quad (4)$$

where the elements p_{ij} are given by

$$p_{ij} = P(X_t = j | X_{t-1} = i) \quad i = 0, 1; \quad j = 0, 1. \quad (5)$$

Nonzero precipitation amounts h_t are simulated here by using the Weibull distribution,

$$F(h) = 1 - \exp \left[- \left(\frac{h}{\alpha} \right)^\beta \right], \quad (6)$$

where α and β are the distribution parameters estimated using maximum likelihood (ML) estimation procedure. To take into account the seasonality of the rainfall process, the parameters were estimated separately for each month.

Stochastic simulation of the series X_t under first-order Markov dependence is straightforward. The output u_t from a uniform [0,1] random number generator is compared with the appropriate transition probability in Equation (3) and a wet day is simulated if the random number is lower than a “critical” probability p_c ,

$$X_t = \begin{cases} 1 & \text{if } u_t \leq p_c \\ 0 & \text{otherwise} \end{cases} \quad \text{with} \quad p_c = \begin{cases} p_{01} & \text{if } X_{t-1} = 0 \\ p_{11} & \text{if } X_{t-1} = 1 \end{cases}. \quad (7)$$

In the present study, transition probabilities are estimated separately for each month of the year. In particular, a time homogeneous Markov chain process is considered for the current scenario, by assuming the occurrence process stationary over the period of observation (i.e., the elements of the monthly transition matrices do not change from year to year).

In addition, a trend analysis is carried out on the annual series of transition probabilities computed for each month. More specifically, a Student's t test for linear trend detection is applied at a significance level $\alpha = 5\%$.

For the future scenarios, monthly transition probabilities are extrapolated by the linear trend function at 2025, if the hypothesis of stationary series is rejected at $\alpha = 5\%$, whereas they are assumed equal to the ones corresponding to the current scenario otherwise.

2.4. Stochastic mean daily temperature generation model

Generation of synthetic mean daily temperature series is carried out by means of an autoregressive moving average (ARMA) model of first order both in the autoregressive and moving average components: that is, ARMA (1,1) model. The readers may refer to Salas (Salas 1992) and references therein for further details on parameter estimation of ARMA (1,1) models.

To handle with seasonality in the original temperature series, the model is applied in normalized form (Bras and Rodriguez-Iturbe 1993),

$$y_t = \phi y_{t-1} + \varepsilon_t - \theta \varepsilon_{t-1}, \quad (8)$$

with

$$y_t = \frac{T_t - \mu_j}{\sigma_j}, \quad (9)$$

where T_t is the mean daily temperature at day t ; μ_j is the mean of the mean monthly temperature values at month j ; σ_j is the standard deviation of the mean monthly temperature values at month j ; and ε_t is the uncorrelated white noise process.

Once that the parameters of the model are estimated, synthetic values of mean daily temperature data can be generated by combining Equations (8) and (9).

2.5. The rainfall-runoff model: IHACRES

The Identification of Unit Hydrographs and Component Flows from Rainfall, Evapotranspiration and Streamflow Data (IHACRES) model (Jakeman et al. 1990; Jakeman and Hornberger 1993; Jakeman et al. 1993; Jakeman et al. 1994a; Jakeman et al. 1994b; Ye et al. 1997) is a simple model designed to perform the identification of hydrographs and component flows purely from rainfall, evaporation, and streamflow data. In IHACRES, the rainfall-runoff processes are represented by two modules: 1) a nonlinear loss module transforms precipitation to effective rainfall by considering the influence of temperature and then 2) a linear module, based on the classical convolution between effective rainfall and an instantaneous unit hydrograph (IUH), provides total streamflow values.

Such a model has been chosen because of its simplicity, parametric efficiency; in particular, daily precipitation, streamflow, and temperature series are the only input data required by the model. The nonlinear loss module involves calculation of an index of catchment storage s_t , based upon an exponentially decreasing weighting of precipitation and temperature conditions,

$$s_t = \frac{r_t}{c} + \left[1 - \frac{1}{\tau_w(T_t)} \right] s_{t-1}, \quad (10)$$

with

$$\tau_w(T_t) = \tau_0 e^{[(20-T_t)/f]}, \quad (11)$$

where s_t is the catchment storage index or catchment wetness/soil moisture index at time t , generally varying from 0 to 1; $\tau_w(T_t)$ is a time constant that is inversely related to the temperature declining rate; τ_0 is the value of $\tau_w(T_t)$ for a reference temperature fixed to a nominal value depending on the climate and usually equal to 20°C for warmer climates; c (mm) is a conceptual total storage volume chosen to constrain the volume of effective rainfall to equal runoff; and f (°C) is a temperature modulation factor. The effective rainfall u_t is computed as the product of total rainfall r_t and the storage index s_t ,

$$u_t = \frac{1}{2}(s_t + s_{t-1})r_t. \quad (12)$$

For the low-yielding catchments (Ye et al. 1997), Equation (12) is modified by introducing two extra parameters p and l to generate u_t , which enables us to take into account the strong nonlinearity caused by the impact of long dry periods on the soil surface. In particular, the loss module is modified as follows:

$$u_t = \left[\frac{1}{2}(s_t + s_{t-1}) - l \right]^p r_t \quad \text{if} \quad \frac{1}{2}(s_t + s_{t-1}) > l$$

$$u_t = 0 \quad \text{otherwise,} \quad (13)$$

where l represents a threshold parameter and p represents the exponent of a power law used to describe the nonlinearity.

Although, in principle, linear convolution of effective rainfall with IUH can be computed for every configuration of conceptual elements (channels or reservoirs) in parallel and/or in a series (Wagener et al. 2004), applications of the original IHACRES model and similar conceptual rainfall–runoff models to low-yielding river basins, as the ones in Mediterranean areas (Ye et al. 1997; Murrone et al. 1997; Candela et al. 2002; Aronica 2007), suggest to use a configuration with one linear channel and two linear reservoirs for a better simulation of the hydrological response.

In the present study, the linear module is implemented by considering the IUH as a combination of one linear channel, corresponding to the quick component of the total streamflow, and two parallel linear reservoirs, corresponding to the slow components (over-day and over-month runoff) of the total streamflow. On the basis of these assumptions, the form of the impulse response derived from the combination of these three linear elements can be expressed as

$$h_t = x_0 \delta(0) + \sum_{i=1}^2 \frac{x_i}{\lambda_i} e^{-(t/\lambda_i)}. \quad (14)$$

The response of the quick component is expressed in the form of Dirac delta function $\delta(t)$, because the catchment time lag is enough smaller than the time interval of data

aggregation and is fed by a fixed percentage of x_0 of effective rainfall. The slow components are expressed with an exponential decay law characterized by the two coefficients λ_1 and λ_2 equal to the inverse of the time constant for the linear reservoirs fed by a fixed percentage of x_1 and x_2 of effective rainfall. Under the hypothesis of linearity, streamflow q at time t is the additive result of the single responses

$$q_t = \sum_{j=1}^t u_j H_{t-j+1} A \Delta t, \quad (15)$$

with

$$H_t = \frac{x_0}{t \Delta t} + \frac{x_1(1 - e^{-(t \Delta t / \lambda_1)})}{t \Delta t} + \frac{x_2(1 - e^{-(t \Delta t / \lambda_2)})}{t \Delta t},$$

$$x_0 + x_1 + x_2 = 1. \quad (16)$$

The model has a total number of 10 parameters: 5 parameters in the nonlinear module (τ_0, f, c, l , and p) and 5 parameters in the linear module (x_0, x_1, x_2, λ_1 , and λ_2).

3. Climate change scenarios

3.1. HadCM3 ocean-atmosphere general circulation model

Expected changes in the future precipitation and mean temperature regimes have been obtained from simulations of the HadCM3 averaged on the nine grid points surrounding Sicily (Figure 3). Then, percentage changes in monthly mean and standard deviation of daily rainfall and mean temperature between a 30-yr control period (1971–2000) and a 25-yr future time slice (2013–37) have been calculated from the model, yielding for each month a population of 900 members for the present and 250 for the future slice.

3.2. Mean monthly precipitation

For the rainfall A2 scenario, the application of the HadCM3 at the case study area shows an overall decreasing trend, as can be observed by the percentage changes of mean daily rainfall (Figure 4, left), clearly pronounced for the summer season, with the only exception of June. This trend is observed, in minor proportion, to the majority of months. An increasing trend is instead reported for January, March, and mainly October, which shows increasing values for the future exceeding 15% at 2025.

On its part, the B2 scenario also shows a pronounced trend of decreasing rainfall in all months and in similar rates, with its maximum negative value in September (over 15%). On the contrary, it displays more humid trends than present for October, November, December, and again January depicts a rise on rainfall regimes. With regard to the standard deviation (Figure 4, right), it seems that the A2 scenario presents a more accentuated variability in the rainfall expected shifts than the B2 scenario, with an overall marked trend to the increase of precipitation variability.



Figure 3. Geographical window considered over Sicily from the HadCM3 global domain (96×73 points) to extract the data related to the climatic variables.

3.3. Mean monthly temperature

Both estimated greenhouse gas emissions scenarios show a continuous rise of mean temperatures, independently of the month (Figure 5, right). In general terms, the temperature raise is more pronounced for the B2 scenario. It is worth observing that, for the B2 scenario, differences between current and future mean temperature greater than 5% occur for February, August, October, November, and December.

With regard to the changes in temperature variability (Figure 5, right), it seems that for the A2 scenario there is a marked increase in summer (e.g., June and July) and a marked decrease in April. The B2 scenario shows less variability for 2025, with the exception of a pronounced increase in October (more than 10%) and decrease in November (more than 15%).

4. Hydrological analysis

On the basis of the procedure outlined in Figure 1, a hydrological analysis through the generation of synthetic rainfall, temperature, and discharge series has

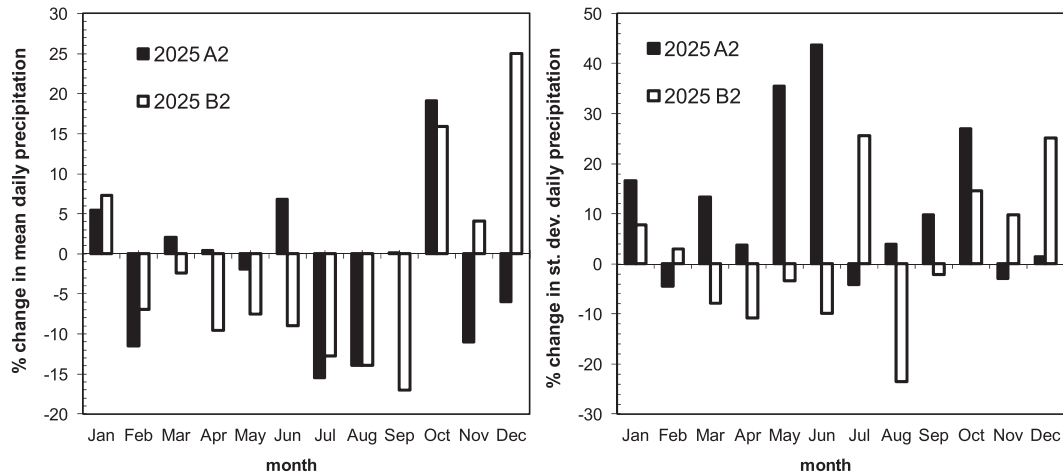


Figure 4. Monthly percentage change of (left) the mean and (right) the standard deviation of daily precipitation for the two scenarios.

been carried out for assessing the current and the future hydropower potential consequent to the climate change scenarios described above.

4.1. Stochastic rainfall generator: Calibration and Monte Carlo generation

The model was calibrated against 40-yr-long (1967–2006) daily rainfall series obtained by spatially averaging the daily data available from three rain gauges within and close to the basin. In Tables 1 and 2, the parameters of Weibull

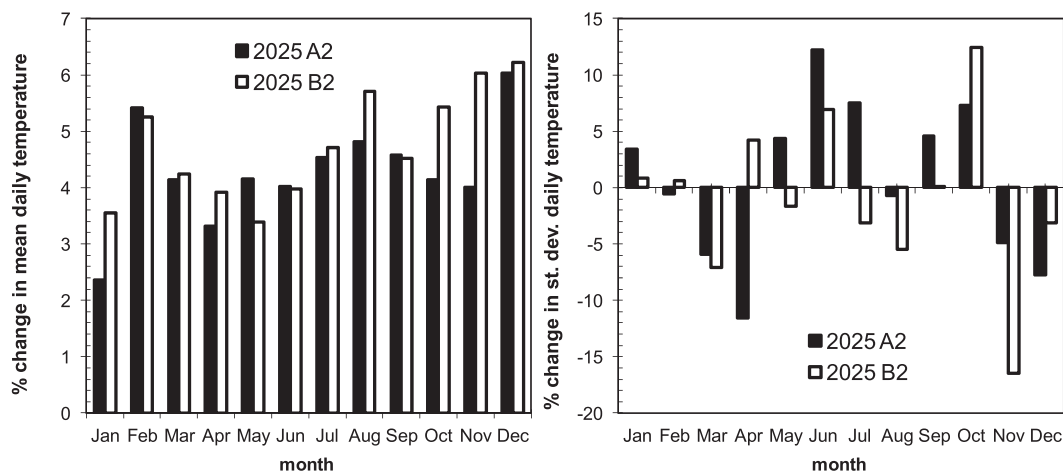


Figure 5. Monthly percentage change of (left) the mean and (right) the standard deviation of daily temperature for the two scenarios.

Table 1. Parameters of Weibull distribution (current scenario).

	Jan	Feb	Mar	Apr	May	Jun	Jul	Aug	Sep	Oct	Nov	Dec
Floresta												
α	11.653	10.773	9.799	10.273	8.980	9.255	10.075	10.914	9.983	10.292	11.367	11.510
β	0.772	0.836	0.875	0.888	0.819	0.879	0.859	0.766	0.837	0.831	1.013	0.784
Francavilla												
α	11.356	10.429	9.589	6.324	6.750	7.509	7.797	8.290	9.167	10.282	9.469	10.209
β	0.630	0.717	0.652	0.645	0.894	1.049	1.033	0.910	0.731	0.545	0.626	0.636
Linguaglossa												
α	14.322	10.924	9.076	7.893	6.776	6.587	7.414	8.066	10.068	13.253	11.238	14.402
β	0.657	0.688	0.569	0.755	0.790	1.189	0.855	0.913	0.715	0.592	0.585	0.661

distribution and the elements of transition probability matrix for the Markov model are reported, respectively.

The new parameters of Weibull distribution for future 2025 scenarios (Tables 3 and 4) have been estimated based on the projected mean and standard deviation of daily rainfall derived by the HadCM3 for the A2 and B2 scenarios. Besides, for the 2025 scenario, monthly transition probabilities, derived as described in section 2.3, are reported in Table 5.

Using those parameters, 1000-yr-long synthetic series have been generated for simulating daily total rainfall for the three scenarios. Figure 6 shows a good agreement between the simulated and observed monthly rainfall depths for the current scenario. Further, Figure 7 shows the generated A2 and B2 scenarios compared with the current scenario (CS) in terms of total monthly rainfall depth. It is worth pointing out how in some months mean daily precipitation shows a variation larger than the one predicted by A2 or B2 scenarios (Figure 6). This is essentially due to the linear trend detected in the monthly transition probabilities at year 2025.

Table 2. Elements of transition probability matrix for the Markov model (current scenario).

	Jan	Feb	Mar	Apr	May	Jun	Jul	Aug	Sep	Oct	Nov	Dec
Floresta												
p_{00}	0.7465	0.7065	0.7596	0.7663	0.8724	0.9230	0.9476	0.9316	0.8404	0.8046	0.7379	0.6981
p_{01}	0.2535	0.2935	0.2404	0.2337	0.1276	0.0770	0.0524	0.0684	0.1596	0.1954	0.2621	0.3020
p_{10}	0.3437	0.3838	0.4212	0.4407	0.5586	0.6485	0.6041	0.5917	0.5457	0.5041	0.4527	0.3555
p_{11}	0.6563	0.6162	0.5788	0.5593	0.4414	0.3515	0.3960	0.4083	0.4543	0.4959	0.5473	0.6445
Francavilla												
p_{00}	0.7779	0.7564	0.7941	0.8427	0.9079	0.9550	0.9736	0.9423	0.8745	0.8422	0.8016	0.7357
p_{01}	0.2221	0.2436	0.2059	0.1573	0.0921	0.0450	0.0264	0.0577	0.1255	0.1578	0.1984	0.2643
p_{10}	0.4704	0.5018	0.5384	0.5140	0.6436	0.7898	0.7255	0.7396	0.5895	0.5355	0.5537	0.4680
p_{11}	0.5296	0.4982	0.4617	0.4860	0.3565	0.2102	0.2745	0.2604	0.4105	0.4645	0.4463	0.5320
Linguaglossa												
p_{00}	0.7749	0.7449	0.7953	0.8184	0.8901	0.9419	0.9606	0.9359	0.8541	0.8190	0.7818	0.7484
p_{01}	0.2251	0.2551	0.2047	0.1816	0.1099	0.0581	0.0394	0.0641	0.1459	0.1810	0.2182	0.2517
p_{10}	0.4574	0.5096	0.5103	0.5424	0.6308	0.8239	0.7888	0.7467	0.6220	0.5549	0.5342	0.4342
p_{11}	0.5426	0.4904	0.4898	0.4576	0.3692	0.1761	0.2112	0.2533	0.3780	0.4451	0.4658	0.5658

Table 3. Parameter of Weibull distribution (2025 A2 scenario).

	Jan	Feb	Mar	Apr	May	Jun	Jul	Aug	Sep	Oct	Nov	Dec
Floresta												
α	11.378	9.067	9.385	10.121	6.761	7.996	7.857	8.048	9.412	11.750	9.731	10.245
β	0.705	0.778	0.793	0.860	0.617	0.672	0.765	0.650	0.769	0.783	0.930	0.733
Francavilla												
α	10.789	8.649	8.834	6.148	5.256	6.869	6.231	6.355	8.509	11.313	7.707	8.899
β	0.581	0.671	0.599	0.628	0.666	0.788	0.913	0.763	0.674	0.520	0.584	0.598
Linguaglossa												
α	13.689	9.021	8.195	7.727	5.027	6.240	5.777	6.186	9.321	14.695	9.071	12.605
β	0.605	0.645	0.526	0.733	0.598	0.883	0.761	0.765	0.660	0.562	0.547	0.621

4.2. Stochastic temperatures generator: Calibration and Monte Carlo generation

The model has been calibrated against an 8-yr-long (1981–88) daily mean temperature series obtained as the average of the daily mean temperature recorded at three thermometric stations within the river basin (Figure 2). Parameters of the model were obtained by ML estimation procedure implemented in a MATLAB routine. Then, 1000-yr-long synthetic series were generated for the three scenarios. Figure 8 shows a good agreement between observed mean daily temperature and simulated data. In addition, Figure 9 shows the generated A2 and B2 scenarios compared with the current scenario in terms of mean monthly temperature. A general increase in temperature values is observed for both 2025 scenarios, as predicted by HadCM3 (Figure 5).

4.3. The IHACRES rainfall-runoff model

Calibration of IHACRES has been carried out by using as input data the spatially averaged daily series of rainfall and air temperature from January 1981 to December 1984 and in comparison with daily flows observed at Alcantara a Moio gauging station (Figure 2) during the same time span. Particularly, the rainfall daily values were averaged over the catchment using Thiessen's polygon method, while the spatially average daily temperature series has been computed using 12 monthly

Table 4. Parameter of Weibull distribution (2025 B2 scenario).

	Jan	Feb	Mar	Apr	May	Jun	Jul	Aug	Sep	Oct	Nov	Dec
Floresta												
α	12.457	9.365	9.863	9.360	8.072	8.479	6.610	10.146	7.384	12.008	11.556	14.371
β	0.768	0.761	0.925	0.900	0.787	0.888	0.622	0.855	0.720	0.840	0.961	0.783
Francavilla												
α	12.124	8.891	9.856	5.794	6.093	6.866	5.516	7.535	6.593	12.071	9.333	12.742
β	0.627	0.657	0.685	0.653	0.857	1.061	0.731	1.023	0.634	0.550	0.599	0.636
Linguaglossa												
α	15.294	9.261	9.433	7.210	6.079	6.016	4.852	7.329	7.206	15.539	11.020	17.976
β	0.655	0.632	0.596	0.764	0.759	1.203	0.619	1.025	0.621	0.597	0.561	0.661

Table 5. Elements of transition probability matrix for the Markov model (2025 scenario).

	Jan	Feb	Mar	Apr	May	Jun	Jul	Aug	Sep	Oct	Nov	Dec
Floresta												
p_{00}	0.4113	0.7065	0.7596	0.7663	0.8724	0.9019	0.9490	0.9316	0.8404	0.8046	0.5842	0.6981
p_{01}	0.5887	0.2935	0.2404	0.2337	0.1276	0.0981	0.0510	0.0684	0.1596	0.1954	0.4158	0.3020
p_{10}	0.2017	0.3838	0.4212	0.4407	0.5586	0.4751	0.5880	0.5917	0.5457	0.5041	0.7181	0.3555
p_{11}	0.7983	0.6162	0.5788	0.5593	0.4414	0.5249	0.4120	0.4083	0.4543	0.4959	0.2819	0.6445
Francavilla												
p_{00}	0.7779	0.6063	0.7941	0.8427	0.9079	0.9550	0.9736	0.9423	0.8745	0.8422	0.8016	0.7357
p_{01}	0.2221	0.3937	0.2059	0.1573	0.0921	0.0450	0.0264	0.0577	0.1255	0.1578	0.1984	0.2643
p_{10}	0.4704	0.8111	0.5384	0.5140	0.6436	0.7898	0.7255	0.7396	0.5895	0.5355	0.5537	0.4680
p_{11}	0.5296	0.1890	0.4617	0.4860	0.3565	0.2102	0.2745	0.2604	0.4105	0.4645	0.4463	0.5320
Linguaglossa												
p_{00}	0.7465	0.4293	0.7596	0.8453	0.8724	0.9230	0.9476	0.9316	0.8404	0.8046	0.7379	0.6981
p_{01}	0.2535	0.5707	0.2404	0.1547	0.1276	0.0770	0.0524	0.0684	0.1596	0.1954	0.2621	0.3020
p_{10}	0.3437	0.7462	0.4212	0.3129	0.5586	0.6485	0.6041	0.5917	0.5457	0.5041	0.4527	0.3555
p_{11}	0.6563	0.2538	0.5788	0.6871	0.4414	0.3515	0.3960	0.4083	0.4543	0.4959	0.5473	0.6445

regression equations of the mean values in each station over the terrain elevation. As a calibration procedure, the generalized likelihood uncertainty estimation (GLUE) (Beven and Binley 1992) has been used here. GLUE is a Monte Carlo technique developed as a methodology for the calibration and estimation of uncertainty of predictive models in equifinality scenarios (Beven 2001).

In the main steps of GLUE procedure, MC sampling was performed by generating 3×10^5 sets of parameters for the model, with each parameter value being drawn from ranges thought feasible for the basin under study. Lacking any prior information about probability distribution of the individual parameters, each one was sampled independently from uniform distributions across the range as proposed by Aronica (Aronica 2007).

Concerning the choice of the goodness-of-fit measure, performance of individual parameter sets has been assessed via a likelihood measure based on the classical Nash and Sutcliffe criterion (Nash and Sutcliffe 1970),

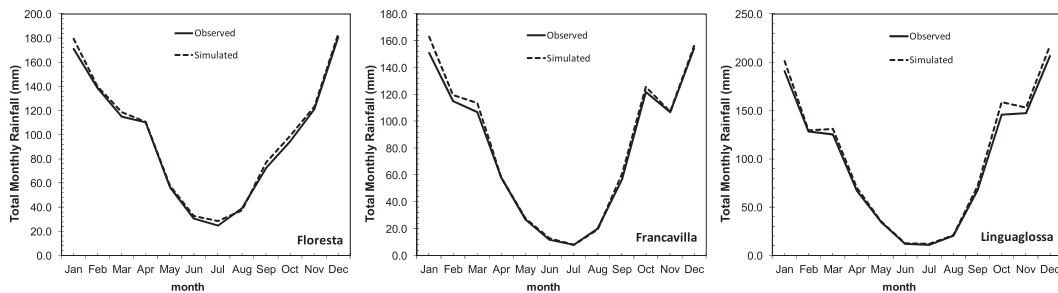


Figure 6. Calibration of the rainfall model: comparison among the observed and simulated monthly rainfall total depths (current scenario).

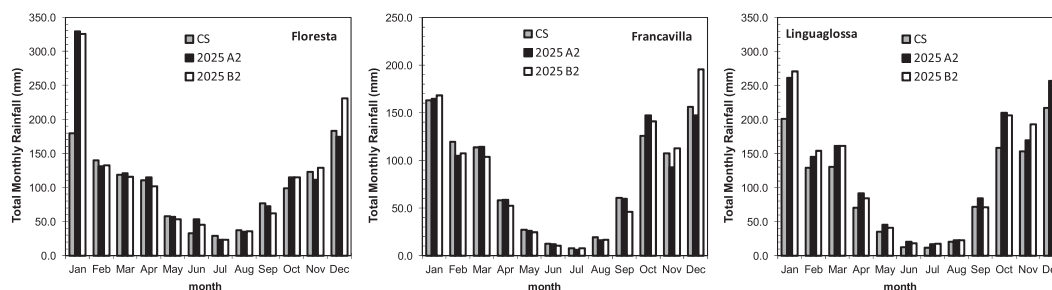


Figure 7. Comparison among the generated A2 and B2 scenarios and the current scenario for monthly rainfall total depths.

$$L(\Theta_i/Y) = (1 - \sigma_i^2/\sigma_{\text{obs}}^2) \quad \sigma_i^2 < \sigma_{\text{obs}}^2, \quad (17)$$

where $L(\Theta_i/Y)$ is the likelihood measure for the i th model simulation for parameter vector Θ_i conditioned on a set of observed daily discharges Y , σ_i^2 is the associated error variance for the i th model, and σ_{obs}^2 is the observed variance for the period under consideration.

Table 6 reports the parameter set values for maximum efficiency in calibration procedure. The maximum efficiency obtained is greater than 0.66 with a significant sensitivity of the parameters and an overall reliability and robustness of the model structure.

These parameter values have been used for modeling the hydrological response of the river basin for the years of calibration and to reconstruct time series of simulated streamflows. Comparison between observed and simulated flow duration curves, streamflow time, and daily discharges series are reported in Figure 10. The good agreement confirms the efficiency of the calibration and the reliability of IHACRES model for this kind of analysis.

4.4. Analysis of hydropower potential

The rainfall and temperature synthetic series were used as input to IHACRES model to generate a 1000-yr-long daily discharge series to be used for hydropower potential analysis.

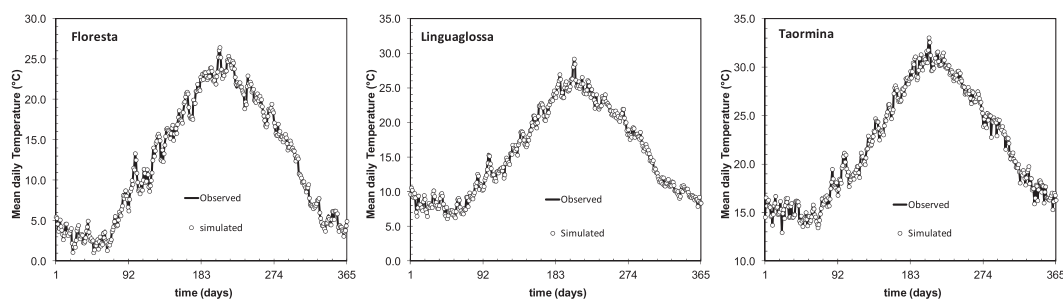


Figure 8. Calibration of the model: comparison among the observed and simulated mean daily temperature (current scenario).

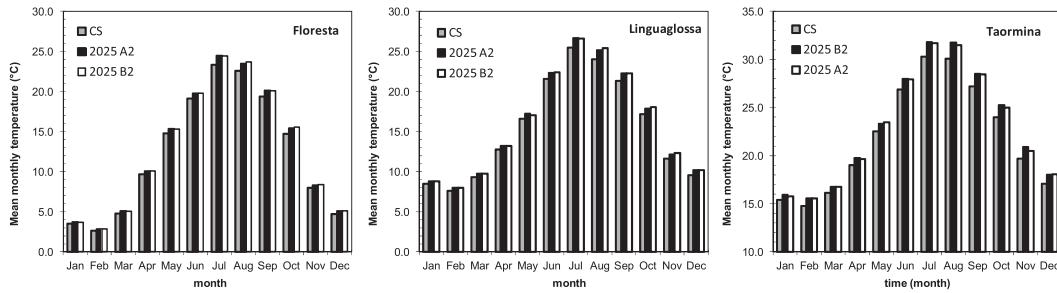


Figure 9. Comparison among the generated A2 and B2 scenarios and the current scenario for daily mean monthly temperature.

First, to check the effectiveness and the reliability of the stochastic procedure, a test was carried out by simply comparing the observed and the generated average flow duration curves for the current scenario. On the left-hand side of Figure 11, the two curves are plotted together showing a quite good agreement. The only discrepancy can be noted in the area under the two curves, which returns the average annual flow. Those volumes result in 81.3 Mm^3 for the observed mean FDC and 109.3 Mm^3 for the generated mean FDC, with a difference of $+34.4\%$. Nevertheless, this circumstance is not significant for the purpose of this study, which is essentially focused on the comparison between the three synthetic scenarios (current, 2025 A2, and 2025 B2).

This latter comparison can be seen on the right-hand side of Figure 11, where the three FDCs for the different scenarios are plotted. The first result to be considered is an increase both in the annual average runoff volume from 109.3 Mm^3 for the current scenario to 127.4 Mm^3 ($+16.6\%$) for the 2025 A2 scenario and to 147.8 Mm^3 ($+35.2\%$) for the 2025 B2 scenario, as well as in the annual average streamflow discharge: that is, from $3.46 \text{ m}^3 \text{ s}^{-1}$ for the current scenario to $4.04 \text{ m}^3 \text{ s}^{-1}$ ($+16.5\%$) for the 2025 A2 scenario and to $4.69 \text{ m}^3 \text{ s}^{-1}$ ($+30.2\%$) for the 2025 B2 scenario. This could be interpreted as an enhancement in the hydrological characteristics of the river to be considered for the future hydroelectric utilizations. In addition, to clarify this point, a new analysis has been carried out using the curve shown in Figure 12. The plot reports the utilization curve that represents a useful tool for designing run-of-rivers hydropower plants. This curve refers to the so-called utilization coefficient, which is defined as the ratio between design discharge and the average annual discharge. This coefficient varies between 0 and 1, depending on the design discharge and FDC, and it represents the derivation rate for the hydropower plant given the hydrological characteristics of the river. To compare the different scenarios, in Figure 12 the utilization coefficient is plotted versus the normalized design discharge (ratio between design discharge and annual average streamflow discharge).

The dashed line in the figure represents the condition of total utilization of the hydropower potential as, along the line, the design discharge is always equal to the

Table 6. Summary results from the GLUE simulations of IHACRES.

Parameters	c (mm)	τ_0 (days)	f (°C)	x_0	x_1	x_2	λ_1 (days)	λ_2 (days)	l	p
Value	679.1	15.94	3.82	0.163	0.277	0.560	12.95	15.51	0.300	0.415

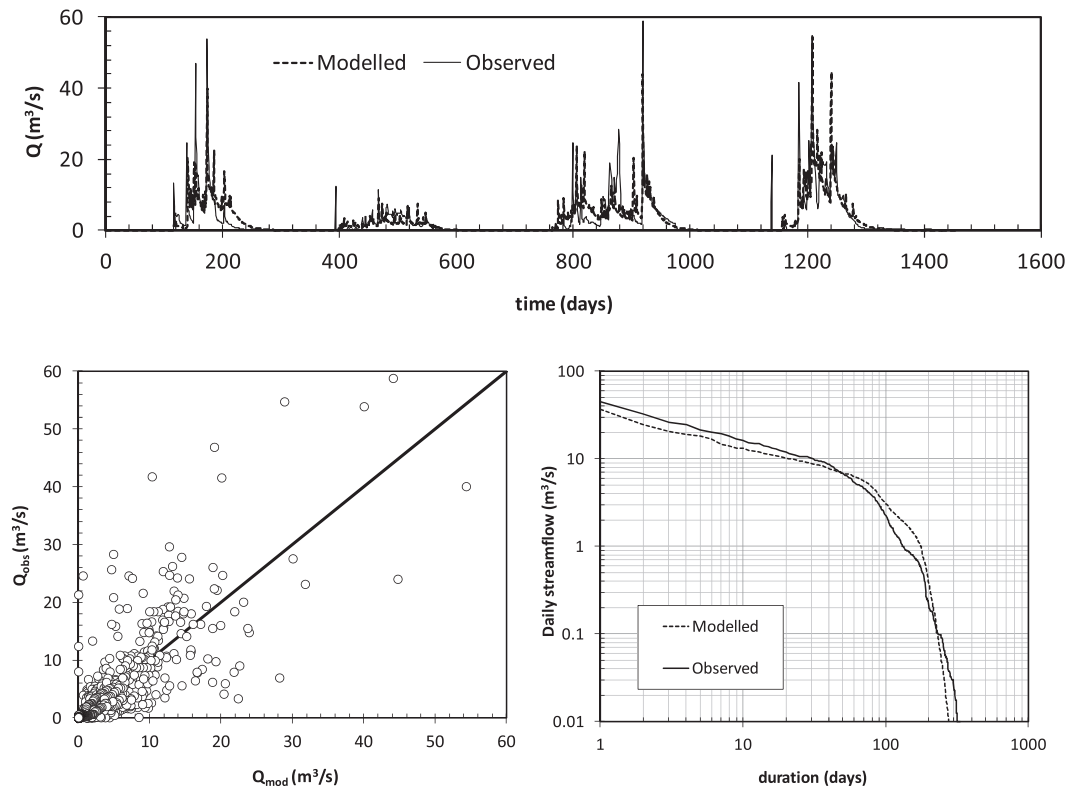


Figure 10. Application of IHACRES to the simulation of Alcantara at Moio stream-flows: (top) observed and modeled daily discharges, (bottom left) Q–Q plot, and (bottom right) modeled and observed flow duration curves.

average annual discharge. The utilization curve is close to this line for perennial flows, whereas it deviates for intermittent flows.

It can be noted how all the curves deviate from the dashed line, as is expected given the hydrological characteristics of the rivers in the Mediterranean area; in addition the analysis of the plot reveals how, for a given design discharge, there is a decrease in the utilization coefficient and hence in the hydropower potential. This reduction is more significant for the A2 2025 scenario than the B2 2025 scenario, despite the difference between the three scenarios being quite small.

5. Conclusions

A preliminary study on the impact of future climate change on the hydrological regime of the Alcantara River basin, eastern Sicily (Italy), oriented to qualitative investigate modifications in the hydropower potential, has been carried out and presented.

Synthetic rainfall, temperature, and runoff series have been generated for the current scenario and two future scenarios at 2025, by combining two stochastic generators of daily rainfall and temperature, respectively, with the IHACRES rainfall–runoff model. In particular, the projected changes in monthly mean and standard deviation values of daily rainfall and temperature, resulting from the application of

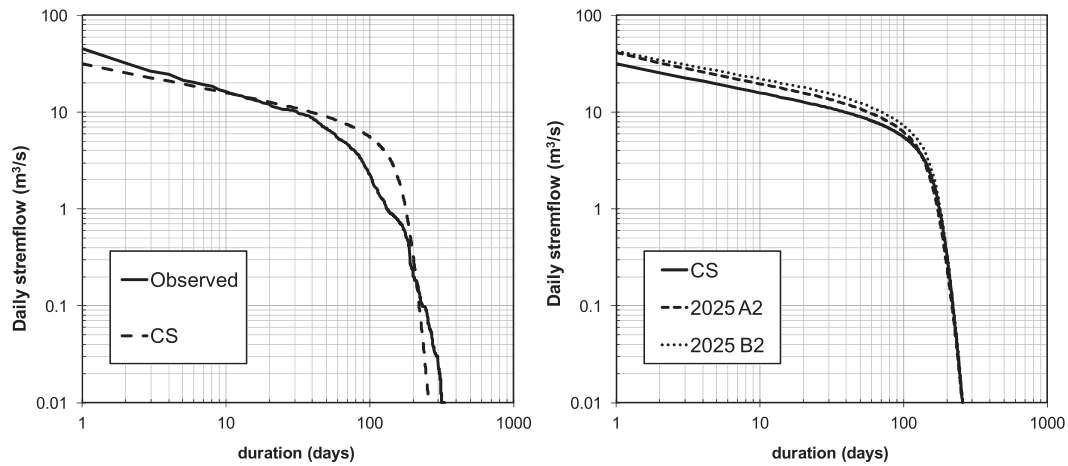


Figure 11. Comparison among flow duration curves (left) for observations and the current scenario and (right) for the future and current scenarios.

the HadCM3, have been adopted to generate future scenarios of precipitation and temperature.

With respect to rainfall series, significantly high values have been computed for some months (e.g., January and December), sometimes in contrast with the HadCM3 projections. This is mainly due to the linear trend detected in the corresponding monthly transition probabilities at year 2025. Also, a general increase in temperature values is observed for both of the 2025 scenarios, in agreement with HadCM3 results.

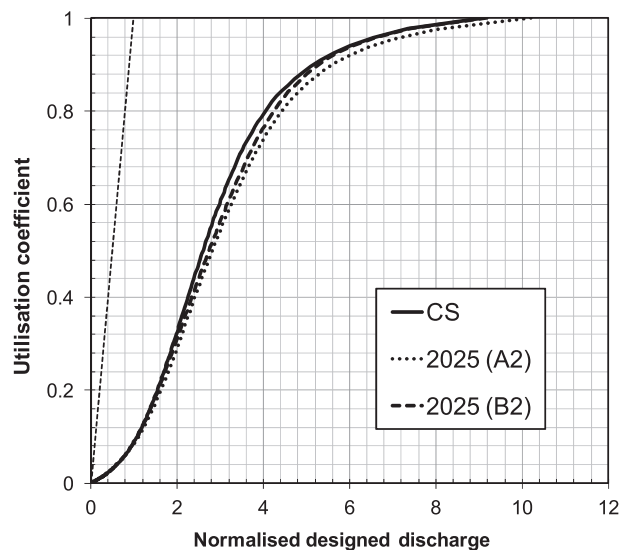


Figure 12. Comparison among utilization curves for the current and future scenarios.

The analysis of flow duration curves returns an increase of the annual average runoff volume as well as of the annual average streamflow discharge for the 2025 considered scenarios. Nevertheless, with reference to streamflow utilization curves, the derived results show a reduction in the utilization coefficient and hence in the hydropower potential, which is more significant for the A2 2025 scenario than for the B2 2025 scenario, despite the differences between the considered scenarios are almost negligible.

It is worth underlying that, since GCMs predictions are uncertain, particularly regarding precipitation, the derived results should be evaluated as indicative of the system's potential response to the considered future climate change scenarios. Nevertheless, such rough estimates of possible future conditions can be considered as a reference frame for decision makers to plan adapting strategies for water resources management.

In addition, because one GCM is hardly sufficient to characterize the possible future outcomes, for the sake of completeness the results here derived by using the HadCM3 projections should be compared with the ones derived by application of other GCMs, although bearing in mind that different GCMs often provide contradicting future scenarios. Ongoing studies are oriented to include the effect of climate change on snowmelting and groundwater recharge for the Etna aquifer.

Acknowledgments. The authors thank FP5 Projects towards Sustainable Water Use on Mediterranean Islands: Addressing Conflicting Demands and Varying Hydrological, Social and Economic Conditions (MEDIS) (EVK1-CT-2001-00092), which were financed by the European Commission. Special thanks are due to A. Amengual, R. Romero, and S. Alonso (Meteorology Group, University of the Balearic Islands).

References

- Aronica, G. T., 2007: Continuous-time modelling of hydrologic time series hydrological conceptual models. *Water Resources Assessment under Water Scarcity Scenarios*, G. La Loggia, G.T. Aronica, and G. Ciruolo, Eds., CSDU, 179–200.
- , C. Corrao, A. Amengual, S. Alonso, and R. Romero, 2005: Water resources evaluation under climatic trend effects in Mediterranean catchments. *Geophys. Res. Abstr.*, **7**, 04091.
- Arora, V. K., and G. J. Boer, 2001: Effects of simulated climate change on the hydrology of major river basins. *J. Geophys. Res.*, **106** (D4), 3335–3348.
- Bates, B. C., Z. W. Kundzewicz, S. Wu, and J. P. Palutikof, 2008: Climate change and water. International Panel on Climate Change Tech. Rep. 6, 214 pp.
- Bernstein, L., and Coauthors, 2007: *Climate Change 2007: Synthesis Report*. IPCC, 104 pp.
- Beven, K. J., 2001: *Rainfall-Runoff Modelling: The Primer*. John Wiley & Sons, 372 pp.
- , and A. M. Binley, 1992: The future of distributed models—Model calibration and uncertainty prediction. *Hydrol. Processes*, **6**, 279–298.
- Bras, R. L., and I. Rodriguez-Iturbe, 1993: *Random Functions and Hydrology*. Dover, 559 pp.
- Candela, A., G. Aronica, and G. Viviani, 2002: Quali-quantitative response of a natural catchment on a daily basis. *Proc. Second Int. Conf. New Trends in Water and Environmental Engineering for Safety and Life: Eco-compatible Solutions for Aquatic Environments*, Capri, Italy, 152–153.
- Candela, L., W. Von Igel, and G. T. Aronica, 2009: Impact assessment of combined climate and management scenarios on groundwater resources and associated wetland (Majorca, Spain). *J. Hydrol.*, **376** (3–4), 510–527.

- Christensen, J. H., and Coauthors, 2007: Regional climate projections. *Climate Change, 2007: The Physical Science Basis*, S. Solomon et al., Eds., Cambridge University Press, 847–940.
- Dibike, Y. B., and P. Coulibaly, 2005: Hydrologic impact of climate change in the Saguenay watershed: Comparison of downscaling methods and hydrologic models. *J. Hydrol.*, **307** (1–4), 145–163.
- Di Marco, S., and A. Licciardello, 2005: Studio preliminare di sistemazione idraulica per la realizzazione di sbarramenti in subalveo a salvaguardia delle risorse idriche superficiali e profonde del fiume Alcantara (in Italian). Ente Parco Fluviale dell’Alcantara Rep., 45 pp.
- Fowler, H. J., M. Ekstroem, S. Blenkinsop, and A. P. Smith, 2007: Estimating change in extreme European precipitation using a multimodel ensemble. *J. Geophys. Res.*, **112**, D18104, doi:10.1029/2007JD008619.
- Gabriel, K. R., and J. Neumann, 1962: A Markov chain model for daily rainfall occurrences at Tel Aviv. *Quart. J. Roy. Meteor. Soc.*, **88**, 90–95.
- Gain, A. K., W. W. Immerzeel, F. C. Sperna Weiland, and M. F. P. Bierkens, 2011: Impact of climate change on the stream flow of the lower Brahmaputra: Trends in high and low flows based on discharge-weighted ensemble modelling. *Hydrol. Earth Syst. Sci.*, **15**, 1537–1545.
- Gordon, C., C. Cooper, C. A. Senior, H. Banks, J. M. Gregory, T. C. Johns, J. F. B. Mitchell, and R. A. Wood, 2000: The simulation of SST, sea ice extents and ocean heat transport in a version of the Hadley Center coupled model without flux adjustments. *Climate Dyn.*, **16**, 147–168.
- Haan, C. T., D. M. Allen, and J. O. Street, 1976: A Markov chain model for daily rainfall. *Water Resour. Res.*, **12**, 443–449.
- Hamlet, A. F., and D. P. Lettenmaier, 2007: Effects of 20th century warming and climate variability on flood risk in the western U.S. *Water Resour. Res.*, **43**, W06427, doi:10.1029/2006WR005099.
- Hanssen-Bauer, I., C. Achberger, R. E. Benestad, D. Chen, and E. J. Førland, 2005: Statistical downscaling of climate scenarios over Scandinavia. *Climate Res.*, **29**, 255–268.
- Jakeman, A. J., and G. M. Hornberger, 1993: How much complexity is warranted in a rainfall-runoff model? *Water Resour. Res.*, **29**, 2637–2649.
- , I. G. Littlewood, and P. G. Whitehead, 1990: Computation of the instantaneous unit hydrograph and identifiable component flow with application to two small upland catchments. *J. Hydrol.*, **117**, 275–300.
- , T. H. Chen, D. A. Post, G. M. Hornberger, I. G. Littlewood, and P. G. Whitehead, 1993: Assessing uncertainties in hydrological response to climate at large scale. *Macroscale Modelling of the Hydrosphere*, W. B. Wilkinson, Ed., IAHS, 37–47.
- , D. A. Post, and M. B. Beck, 1994a: From data and theory to environmental model: The case of rainfall-runoff. *Environmetrics*, **5**, 297–314.
- , —, S. Y. Schreider, and W. Ye, 1994b: Modelling environmental systems: Partitioning the water balance at different catchment scales. *Environmental Studies*, Vol. 2, *Computer Techniques in Environmental Studies V*, P. Zannetti, Ed., Computational Mechanics, 157–170.
- Johns, T. C., and Coauthors, 2003: Anthropogenic climate change for 1860 to 2100 simulated with the HadCM3 model under updated emissions scenarios. *Climate Dyn.*, **20**, 583–612.
- Kunstmann, H., and C. Stadler, 2005: High resolution distributed atmospheric hydrological modelling for alpine catchments. *J. Hydrol.*, **314**, 105–124.
- , K. Schneider, R. Forkel, and R. Knoche, 2004: Impact analysis of climate change for an alpine catchment using high resolution dynamic downscaling of ECHAM4 time slices. *Hydrol. Earth Syst. Sci.*, **8**, 1031–1045.
- Mays, L. W., 2001: *Water Resources Engineering*. John Wiley & Sons, 768 pp.
- Mirza, M. M. Q., 2002: Global warming and changes in the probability of occurrence of floods in Bangladesh and implications. *Global Environ. Change*, **12**, 127–138.
- Murrone, F., F. Rossi, and P. Claps, 1997: Conceptually-based shot noise modelling of streamflows at short time interval. *Stoch. Hydrol. Hydraul.*, **11**, 483–510.
- Nakícenović, N., 2000: Greenhouse gas emissions scenarios. *Technol. Forecast. Soc. Change*, **65**, 149–166.

- Nash, J. E., and J. V. Sutcliffe, 1970: River flow forecasting through conceptual models. Part I—A discussion of principles. *J. Hydrol.*, **27**, 282–290.
- Pope, V. D., M. L. Gallani, P. R. Rowntree, and R. A. Stratton, 2000: The impact of new physical parametrizations in the Hadley Centre climate model: HadAM3. *Climate Dyn.*, **16**, 123–146.
- Prudhomme, C., and H. Davies, 2009: Assessing uncertainties in climate change impact analyses on the river flow regimes in the UK. Part 1: Baseline climate. *Climatic Change*, **93**, 177–195.
- Quintana Seguí, P., A. Ribes, E. Martin, F. Habets, and J. Boé, 2010: Comparison of three downscaling methods in simulating the impact of climate change on the hydrology of Mediterranean basins. *J. Hydrol.*, **383**, 111–124.
- Salas, J. D., 1992: Analysis and modeling of hydrologic time series. *Handbook of Hydrology*, D. R. Maidment, Ed., McGraw-Hill, 19.1–19.72.
- Senatore, A., G. Mendicino, G. Smiatek, and H. Kunstmann, 2011: Regional climate change projections and hydrological impact analysis for a Mediterranean basin in southern Italy. *J. Hydrol.*, **399**, 70–92.
- Stern, R. D., and R. Coe, 1984: A model fitting analysis of daily rainfall data (with discussion). *J. Roy. Stat. Soc.*, **147A**, 1–34.
- Teutschbein, C., and J. Seibert, 2012: Bias correction of regional climate model simulations for hydrological climate-change impact studies: Review and evaluation of different methods. *J. Hydrol.*, **456–457**, 12–29, doi:10.1016/j.jhydrol.2012.05.052.
- Thornthwaite, C. W., 1948: An approach toward a rational classification of climate. *Geogr. Rev.*, **38**, 55–94.
- Todorovic, P., and D. A. Woolhiser, 1976: Stochastic structure of the local pattern of precipitation. *Stochastic Approaches to Water Resources*, Vol. 2, H. W. Shen, Ed., Water Resources Publications, 15.1–15.37.
- Wagener, T., H. S. Wheater, and H. V. Gupta, 2004: *Rainfall-Runoff Modelling in Gauged and Ungauged Catchments*. Imperial College Press, 306 pp.
- Waymire, E., and V. K. Gupta, 1981: The mathematical structure of rainfall representations, 1. A review of the stochastic rainfall models. *Water Resour. Res.*, **17**, 1261–1272.
- Wilby, R. L., S. P. Charles, E. Zorita, B. Timbal, P. Whetton, and L. O. Mearns, 2004: Guidelines for use of climate scenarios developed from statistical downscaling methods. IPCC Task Group on Data and Scenario Support for Impact and Climate Analysis Rep., 27 pp.
- Wilks, D. S., 1998: Multisite generation of daily stochastic precipitation generation model. *J. Hydrol.*, **210**, 178–191.
- Xu, C., 1999: Climate change and hydrologic models: a review of existing gaps and recent research developments. *Water Resour. Manage.*, **13**, 369–382.
- Ye, W., B. C. Bates, N. R. Viney, M. Sivapalan, and A. J. Jakeman, 1997: Performance of conceptual rainfall-runoff models in low-yielding ephemeral catchments. *Water Resour. Res.*, **33**, 153–166.